Low Temperature Physics/Fizika Nizkikh Temperatur, 2020, v. 46, No. 7, pp. 837–844

Resonance properties of magnetic helical structures

A.S. Kovalev

B. Verkin Institute for Low Temperature Physics and Engineering of the National Academy of Sciences of Ukraine
47 Nauky Ave., Kharkiv 61103, Ukraine

V.N. Karazin Kharkiv National University, 4 Svobody Sq., Kharkiv 61077, Ukraine
E-mail: kovalev@ilt.kharkov.ua

Received March 16, 2020, published online May 26, 2020

The dependence for the frequencies of the internal modes on the external field in spiral structures in easy-plane antiferromagnets with a small in-plane anisotropy are studied theoretically in a wide region of the fields including the spin-flop transition field. The theoretical results are compared with the known experimental data for the antiferromagnetic resonance in $NdFe_3(BO_3)_4$. This comparison enabled to reconstruct the dependence for the spiral period of the magnetic structure on the external field.

Keywords: antiferromagnet, antiferromagnetic resonance, helix, excitation modes.

1. Introduction

The complicated magnetic structures with a spiral (helical) or transverse-spiral (cycloidal) modulation of magnetization along a specific crystallographic direction have been actively studied in recent years, both theoretically and experimentally. Such helimagnets are ubiquitous in the field of magnetism. The reason for an existence of the helical structures may be connected with either Dzyaloshinskii–Moriya or competing exchange interactions. They appear either in the most multiferroics [1], or as a result of a competition of different physical field (with a several order parameters), for example, between magnetization and polarization. Spirals in multiferroics have attracted a great attention for applications based on their control with electric and magnetic fields [2]. Particularly the properties of multiferroics of the $RFe_3(BO_3)_4$ family of ferroborates with different rare-earth ions R^{3+} have recently been under active study due to large magnetoelectric effect [3]. In this paper, the author reports some theoretical results about the general features concerning to the resonant properties of the spiral structures with an application to the particular case of $NdFe_3(BO_3)_4$. This compound was actively studied experimentally [4,5]. It has a number of interesting physical properties, including magnetic ordering of different magnetic sublattices, incommensurability of the magnetic structure and spontaneous polarization **P**.

The compound $NdFe_3(BO_3)_4$ has a crystal structure with trigonal space group $R32$. The main feature of the crystal structure is that distorted FeO_6 octahedral form spiral chains with threefold screw-axis symmetry along the crystallographyc c axes. The lattice parameter in c direction (Z axis) $c = 7.603$ Å corresponds to the minimal distance between the neighboring Fe^{3+} ions $R_{FF} = a = c/2 = 3.8$ Å, and the parameter in a direction (X axis in Fig. 1a) is $\delta = 9.594$ Å [6,7]. The crystallographic spiral (see Fig. 1b) is short-periodic with $L_c \approx 3R_{FF}$. The structure of the compound is represented in Fig. 1. Equal-size dark (red) circles in Fig. 1a corresponds to the Fe^{3+} ions and clear (green) circles to Nd^{3+} ions in the same XY plane perpendicular to Z axis.

Magnetic properties of the $NdFe_3(BO_3)_4$ are formed by two magnetic sublattices of Fe^{3+} with spin $S = 5/2$ and Nd^{3+} with spin $S = 3/2$ at low temperatures [8]. The main superexchange (through the oxygen ions) antiferromagnetic interaction between Fe^{3+} along the chains (between the nearest planes in Fig. 1) is equal to $J \approx -277$ kOe for the magnetic Hamiltonian of the system [9]:

$$E = -J\sum_{n,m} S_n S_m - J_2 \sum_{n,\mu} S_n S_\mu - J_{FN} \sum_{n,s} S_n J_s + D/2 \sum_n J_n^2, \tag{1}$$

where S_n is the momentum of Fe^{3+} and J_n for Nd^{3+}.

The 2nd nearest-neighbor interaction between Fe^{3+} in Fe-subsystem (in the same plane in Fig. 1) is much smaller: $J_2 \approx -31$ kOe [9]. Interionic Fe–Nd interaction is much smaller and ferromagnetic one: $J_{FN} \approx +4.5$ kOe. But this interaction is very important by the following reason: magnetic anisotropy of Fe^{3+} ions is absent and only easy-plane anisotropy with additional in-plane anisotropy of Nd^{3+} moment which is related to the crystal field of Nd^{3+} ion with a six-fold symmetry exists and has the value

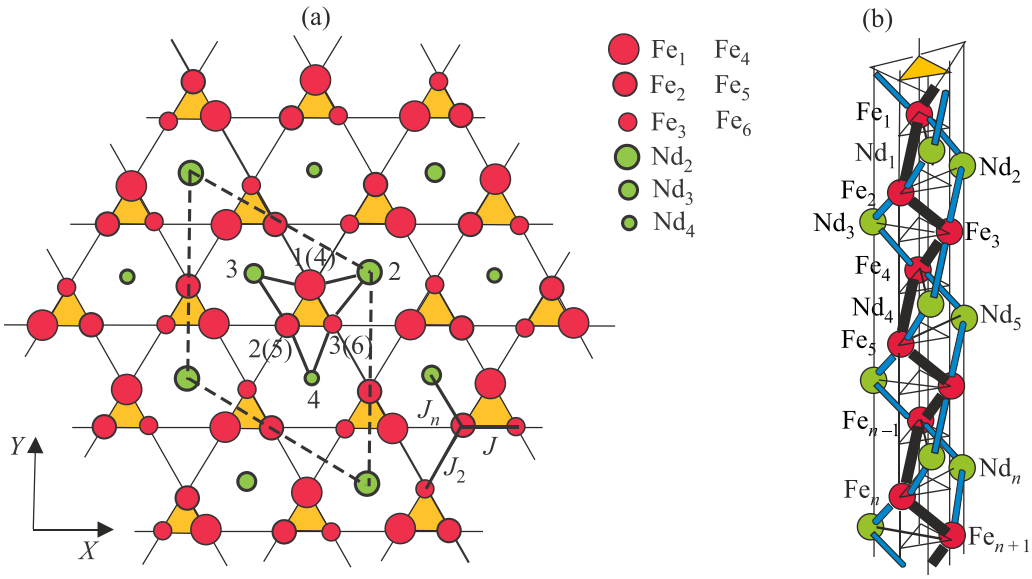

Fig. 1. (Color online) Crystallographyc structure of $NdFe_3(BO_3)_4$ in *XY* plane (a) and along Z direction (b).

$D \approx 13.43$ kOe [9]. Owing to the Fe–Nd exchange interaction this anisotropy reduces to the effective magnetic anisotropy in the main magnetic chain of Fe^{3+}. As a result of these magnetic interactions, below the Néel temperature $T_N \approx 30.6$ K an antiferromagnetic ordering of the iron magnetic subsystem develops in the easy *XY* plane. The neodymium subsystem has no its own phase transition but orders by the Fe–Nd exchange interaction. The different types of magnetic ordering obtained from the neutron experiments are proposed in [7–10] and the most probable one is represented in Fig. 2a. In each atomic layer in *XY* plane, all the ion moments are ferromagnetic ordered, but moments of the neighboring layers are antiferromagnetic-aligned. By reason of the threefold screw-axis symmetry, the ground state represents the domain structure with three types of domains with different orientations. But in a small magnetic field of the order of 2 kOe, the crystal becomes monodomain one. This collinear structure exists in temperature interval $13.5\ \text{K} < T < 30.5\ \text{K}$. At $T_c \approx 13.5$ K another phase transition takes place in which an incommensurate helical magnetic structure develops in the direction of the *c* axis [7]. This structure is represented qualitatively in Fig. 2(b). In reality, the spiral has a long-periodic form and the period of spin helix decreases from $L \approx 3900$ Å at 14 K to $L \approx 1123$ Å at 2 K, i.e. $L >> c$ [10]. The Fourier analysis of the spiral structure demonstrates small but visible third-order harmonics [7]. So the helix has a nonlinear structure, but it is not "a magnetic soliton lattice": magnetic length $\Lambda = c\sqrt{J/\beta_1}$ (where β_1 is the small anisotropy in the easy plane) is of the order of $\Lambda \approx 85c \sim L \approx 150c$.

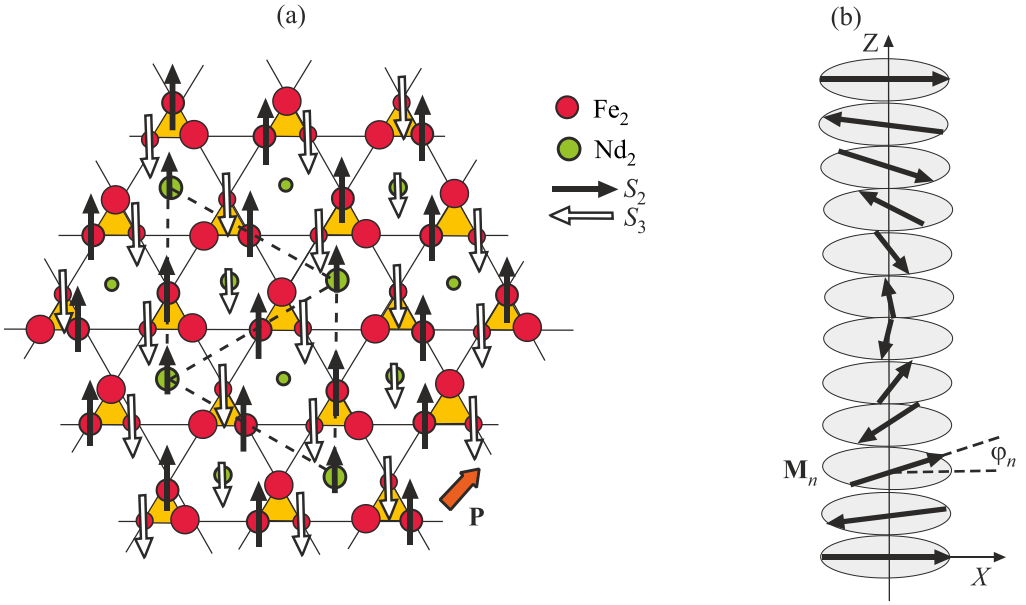

Fig. 2. (Color online) Magnetic structure of $NdFe_3(BO_3)_4$ in collinear phase at $T_c < T < T_N$ (a) and in incommensurate helical structure at $T < T_c$ (b).

Below Néel temperature an antiferromagnetic ordering induces magnetostriction and appearance of a weak spontaneous polarization in the XY plane (red arrow **P** in Fig. 2a) which increases linearly as the temperature is lowered to $T \sim 19$ K [11]. Below $T = 19$ K in the temperature region of spiral phase existence the dependence $P = P(T)$ changes essentially [11] and this fact demonstrates the fundamental connection between the polarization and chiral properties of the $NdFe_3(BO_3)_4$. In the external magnetic field at low temperatures ($T = 4.5$ K) polarization is oriented along the field and rapidly increases from 10 μC/m^2 to 400 μC/m^2 at $H \approx 10$ kOe (the field of the spin-flop phase transition) [12].

2. Experimental results

Investigation of resonance properties of a family of ferroborates gives additional information about magnetic structure, magnetic constants and behavior in magnetic field for these compounds. Theoretically antiferromagnetic resonance (AFMR) was studied in the framework of classical Landau–Lifshitz equations for two-sublattice antiferromagnets (AFM) [13,14]. In the simplest model of two-sublattice AFM in homogeneous magnetic field we consider the following classical energy of elementary magnetic cell in a spatial uniform state:

$$E = J\,\mathbf{M}_1\mathbf{M}_2 + \beta\left(\left(\mathbf{M}_1\mathbf{n}_z\right)^2 + \left(\mathbf{M}_2\mathbf{n}_z\right)^2\right)/2 -$$

$$-\beta_1\left(\left(\mathbf{M}_1\mathbf{n}_x\right)^2 + \left(\mathbf{M}_2\mathbf{n}_x\right)^2\right)/2 - \left(\mathbf{M}_1 + \mathbf{M}_2\right)\mathbf{H}, \qquad (2)$$

where J is the exchange interaction between nearest-neighbor magnetic moments of the Fe layers, $\mathbf{M}_i$ are the magnetization per one magnetic chain, β is a constant of the main magnetic easy-plain anisotropy, $\beta_1 << \beta$ is the constant of the additional small anisotropy in this easy-plain (X is the easy direction in XY plane), $\mathbf{H} = M_0\mathbf{h}$ is the external magnetic field in easy plane (M_0 is the nominal magnetization of the sublattice), $\mathbf{n}_z$ and $\mathbf{n}_x$ are the units vectors along the corresponding axes. In the framework of Landau–Lifshitz equations this Hamiltonian results in the resonance dependences of the eigenmodes of the system, which are depicted in Fig. 3a. Thick lines in Fig. 3a are for the field directed along the easiest direction (X in Fig. 1a), thin lines are for the perpendicular field in Y direction. Spin-flop transition takes place in the field $h_{sf} = \sqrt{(2J+\beta_1)\beta_1}$. The characteristic resonance frequencies at zero field are given by expressions

$$\Omega_1 = gM_0\sqrt{(2J+\beta+\beta_1)\beta_1},$$

$$\Omega_2 = gM_0\sqrt{(2J+\beta_1)(\beta+\beta_1)},$$

where g is the gyromagnetic ratio. In strong fields $\omega \approx gH$. The magnetic parameters of $NdFe_3(BO_3)_4$ were measured by AFMR method [4] and, as a result, the following resonance frequencies were obtained: the high-frequency AFMR branch was observed at frequency $\Omega_2 = 101.9$ GHz and low-frequency branch at $\Omega_1 = 23.8$ GHz. With $J = 580$ kOe [15] ($J = 574$ kOe in [6]) it follows from above mentioned formulas the value of spin-flop field $H_{sf} \approx 8.84$ kOe (in the experiment [16] $H_{sf} \approx 10$ kOe) and the anisotropy values: $\beta = 1.14$ kOe and $\beta_1 = 0.06$ kOe [4]. (The last constant is higher than calculated in [15] $\beta_1 = 0.012$ kOe for the three-fold screw-axis symmetry case.)

It seems that for the fixed direction of the external magnetic field in the easy plane the spiral structure can be explained by the fact that in spiral phase the magnetic structure consists of alternating segments with the antiferromagnetic vector oriented parallel and perpendicular to the external field; in each of these, the field dependence of the frequency is described by curves in Fig. 3a (thin lines in Fig. 3b). Then the complete collection of resonance dependences for the eigenmodes must include both the sets of frequencies for $\mathbf{H}_{\|}$ and $\mathbf{H}_{\perp}$ in Fig. 3a. But the experiments [4,5] demon-

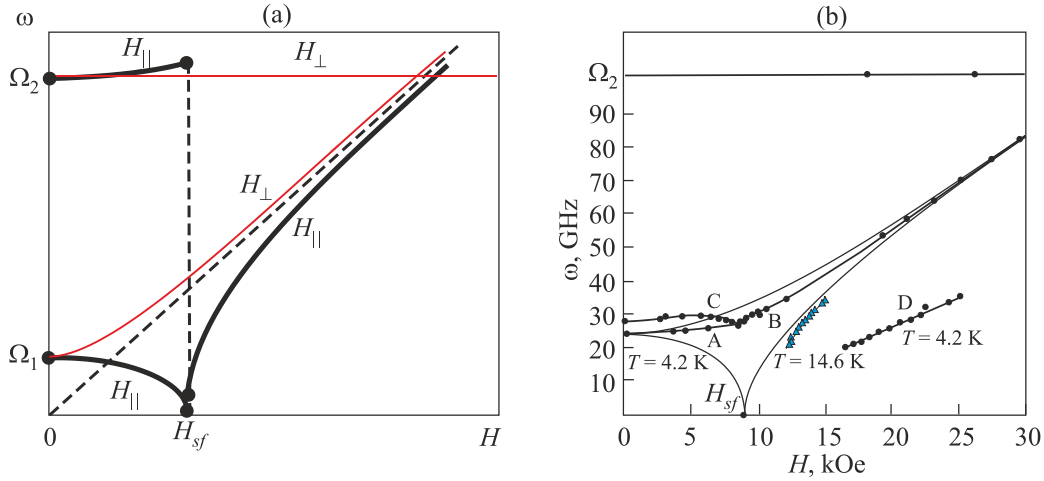

Fig. 3. Theoretical frequency-field dependences of AFMR spectrum for the external magnetic fields in the collinear phase (a), experimental data for these dependences in the field parallel to the easy axis in the spiral phase (b).

strate quite different structure of AFMR frequencies pattern. In Fig. 3b this pattern is represented for the case of the external field directed in the easy axis. Some dependences (A and B) are situated between the lines for the collinear structure, but two unusual resonance curves appear (C and D in Fig. 3b). An additional absorption line (C) is observed within a narrow frequency interval $27\ \text{GHz} < \omega < 30\ \text{GHz}$ [5]. This resonance absorption is observed only when the stationary external field is raised and the additional absorption peak does not show up when the field is lowered. Another absorption peak (D) is observed in field interval $15\ \text{kOe} < h < 25\ \text{kOe}$ with the essential shift from the dependence for the collinear phase (triangles in Fig. 3b).

3. Theoretical model

We examine the resonance properties of the spiral system in the incommensurate phase in the simplest case of zero temperature and without damping in the simplest model with the energy of the unit cell (2). The total energy of spatial inhomogeneous states can be written as

$$E=\sum_n J\left(\mathbf{M}_1^{(n)}\mathbf{M}_2^{(n)}/2+\left(\mathbf{M}_1^{(n)}\mathbf{M}_2^{(n+1)}+\mathbf{M}_2^{(n)}\mathbf{M}_1^{(n-1)}\right)/4\right)+$$

$$+\sum_n\left(\mathbf{M}_1^{(n)}\mathbf{H}+\mathbf{M}_2^{(n)}\mathbf{H}\right)+\sum_n\beta\left(\left(\mathbf{M}_1^{(n)}\mathbf{n}_z\right)^2+\left(\mathbf{M}_2^{(n)}\mathbf{n}_z\right)^2\right)/2-$$

$$-\sum_n\beta_1\left(\left(\mathbf{M}_1^{(n)}\mathbf{n}_x\right)^2+\left(\mathbf{M}_2^{(n)}\mathbf{n}_x\right)^2\right)/2. \qquad (3)$$

After a symmetrization of this expression, introducing the dimensionless vector of one-cell magnetization $\mathbf{m}=\left(\mathbf{M}_1+\mathbf{M}_2\right)/2M_0$ and antiferromagnetism vector $\mathbf{l}=\left(\mathbf{M}_1-\mathbf{M}_2\right)/2M_0$, assuming the condition $m \ll l$ in long-wave approximation we obtain the density of following energy:

$$W\approx 2JM_0^2m^2+JM_0^2a^2\left(d\mathbf{l}/dz\right)^2-2M_0^2\left(\mathbf{hm}\right)^2+$$

$$+\beta M_0^2\left(\mathbf{l}\mathbf{n}_z\right)^2-\beta_1M_0^2\left(\mathbf{l}\mathbf{n}_x\right). \qquad (4)$$

We are interested in AFMR with low frequencies which are much smaller than the frequency of exchange mode $\omega \sim J$. In this limit the magnetic energy density of the system (4) results in dynamical equations [17]:

$$\left[\mathbf{l}\mathbf{l}_{tt}\right]/\left(gM_0\right)^2-2J^2a^2\left[\mathbf{l}\mathbf{l}_{zz}\right]+2\mathbf{l}_t\left(\mathbf{lh}\right)/\left(gM_0\right)+\left[\mathbf{lh}\right]\left(\mathbf{lh}\right)+$$

$$+2J\beta\left[\mathbf{l}\mathbf{n}_z\right]\left(\mathbf{l}\mathbf{n}_z\right)-2J\beta_1\left[\mathbf{l}\mathbf{n}_x\right]\left(\mathbf{l}\mathbf{n}_x\right)=0. \qquad (5)$$

These approximate equations give the values of characteristic frequencies in the collinear phase $\Omega_1\approx gM_0\sqrt{2J\beta_1}$ and $\Omega_2=gM_0\sqrt{2J\left(\beta+\beta_1\right)}$ which are close to the exact above-mentioned frequencies. In this approximation, the frequencies of AFMR in collinear phase satisfy the equation

$$\left(\omega^2-2J\left(\beta+\beta_1\right)+h^2\right)\left(\omega^2-2J\beta_1+h^2\right)-4\omega^2h^2=0, \qquad (6)$$

where $\omega=\Omega/gM_0$. In small fields $h<h_{sf}$ two branches of AFMR have the field dependences:

$$\omega_1\approx\sqrt{2J\beta_1-h^2}\,,\ \omega_2\approx\sqrt{2J\left(\beta+\beta_1\right)+3h^2}\,, \qquad (7)$$

which are depicted in Fig. 3b by thin lines.

In the incommensurate spiral phase for static case, vector $\mathbf{l}$ lies in the easy plane and rotates in that plane; its components are $l_x=l\cos\varphi$ and $l_y=l\sin\varphi$ with the polar angle (see Fig. 2b) is counted from the direction of the a axis and obeys the equation

$$2J^2a^2\varphi_{zz}-\left(2J\beta_1-h^2\right)\sin\varphi\cos\varphi=0. \qquad (8)$$

Although there are no longer any pure collinear and spin-flop structures in the helical phase, when the field passes through $h_{sf}\approx\sqrt{2J\beta_1}$ the solutions of Eq. (8) change considerably:

$$\varphi_1=\pi/2+\mathrm{am}\left(\sqrt{1-(h/h_{sf})^2}\,z/\Lambda k,k\right),\ h<h_{sf}, \qquad (9)$$

$$\varphi_2=\mathrm{am}\left(\sqrt{(h/h_{sf})^2-1}z/\Lambda k,k\right),\ \ h>h_{sf}, \qquad (10)$$

where $\mathrm{am}(pz,k)$ with $p=\sqrt{1-(h/h_{sf})^2}/\Lambda k$ is the Jacobi elliptic amplitude, and $0\le k\le 1$ is its modulus. The period of the incommensurate structure (of the function $l_x^2(z)$) is

$$L=\Lambda 2kK(k)/\sqrt{\left|1-(h/h_{sf})^2\right|}, \qquad (11)$$

where $K(k)$ is the complete elliptic integral of the first kind. In zero field, substituting the experimental data for a, J, β_1 and L in this expression yields $k\approx 0.812$. Thus, no distinct soliton structure is observed. Nevertheless, qualitatively we can interpret the solution (9), (10) as alternating regions of a collinear phase with $\mathbf{l}\parallel\mathbf{n}_x$ and length L separated by kinks (domain walls) in a spin-flop phase with $\mathbf{l}\parallel\mathbf{l}_y$. The solution for φ_2 describes alternating domains of a spin-flop phase with $\mathbf{l}\parallel\mathbf{n}_y$ separated by kinks in a collinear phase with $\mathbf{l}\parallel\mathbf{n}_x$.

Unfortunately, there are no experimental data about changing of the spiral structure in the external field. But magnetization measurement at low values of the magnetic field show some features at $H\sim 10$ kOe, i.e., at the spin-flop field [10]. Some information about the helix structure can be obtained from the results of AFMR experiments from [4,5]. They show the existence of two AFMR branches in the frequency interval 23.8–30 kOe and the absence of any branches in frequency interval 19–23.8 kOe in small fields $H<16$ kOe (see Fig. 3b). We will study below the possible scenarios of the helix transformation with the field taking in mind these facts.

4. Resonant properties of spiral structure in the field $h < h_{sf}$

Let us examine the spiral structure in the fields $h < h_{sf}$. Linearizing Eq. (5) with respect to the static helicoid structure Eq. (9), i.e., taking $\varphi(z,t) = \varphi_1(z) + \phi(z,t)$, with $\phi << 1$, and $\vartheta << 1$, where ϑ is the angle of the deviation for vector **l** out of the easy plane, for small oscillations we obtain the equations

$$\vartheta_{tt}/(gM_0)^2 - 2J^2a^2\vartheta_{zz} + \Big[2J\beta - 2J^2a^2\varphi_z^2 + \\ + \cos^2\varphi(2J\beta_1 - h^2)\Big]\vartheta - 2h/(gM_0)\cos\varphi\phi_t = 0, \quad (12)$$

$$\phi_{tt}/(gM_0)^2 - 2J^2a^2\phi_{zz} + \Big[-(2J\beta_1 - h^2) + \\ + 2(2J\beta_1 - h^2)\cos^2\varphi\Big]\phi + 2h/(gM_0)\cos\varphi\vartheta_t = 0. \quad (13)$$

We will be interested in low-frequencies branches of the AFMR spectrum ($\omega << J$) for which Eqs. (12), (13) can be simplified. For these branches $\partial/\partial t \sim gM_0\sqrt{J\beta_1}$ and $\partial/\partial z \sim \sqrt{\beta_1/Ja^2}$, and in the main approximation, it follows from Eq. (12)

$$\vartheta \approx h\cos\varphi\phi_t/(J\beta gM_0), \quad (14)$$

and Eq. (13) modifies

$$\phi_{tt}/(gM_0)^2 - 2J^2a^2\phi_{zz} + \Big[-(2J\beta_1 - h^2) + \\ + 2(2J\beta_1 - h^2)\cos^2\varphi\Big]\phi = 0. \quad (15)$$

For the small oscillations of the form $\phi = u(z)\sin\Omega t$ in the case of incommensurate structure (9), (10) we get the equation

$$2J^2a^2u_{zz} + \\ + \Big[(\omega^2 + (2J\beta_1 - h^2)) - 2(2J\beta_1 - h^2)\mathrm{sn}^2(pz,k)\Big]u = 0. \quad (16)$$

In experiments with the spatially uniform magnetic field only the homogeneous excitations with the frequencies, which correspond to the bounds of spin waves bands (bounds of the spectrum gap), are excited. The periodic solutions of Eq. (16), which correspond to these excitations, are well known [18]:

$$u_- = \mathrm{cn}(pz,k),\ \omega_- = \omega_0\sqrt{1-(h/h_{sf})^2}\,k'/k, \quad (17)$$

$$u_+ = \mathrm{sn}(pz,k),\ \omega_+ = \omega_0\sqrt{1-(h/h_{sf})^2}\,/k, \quad (18)$$

where the additional modulus $k' = \sqrt{1-k^2}$, $\mathrm{cn}(pz,k)$, and $\mathrm{sn}(pz,k)$ are the Jacobi elliptic cosine and sine, $\omega_0 = \sqrt{2J\beta_1}$ is the frequency at $h = h_{sf}$ (in the triple point ABC in Fig. 3b with experimental value $\omega_0 \approx 27.6$ GHz). For the fixed period of the spiral $L = \mathrm{const}$ (and so for $k = \mathrm{const}$) in the limit $h \to h_{sf}$ both the frequencies $\omega_\pm$ from Eqs. (17), (18) tend to zero. But the experiments [4,5] demonstrate the absence of any AFMR absorption for $\omega < 23.8$ GHz in this area of the field. So the period of the structure depends on the value of the external field: $L = L(h)$ and $k = k(h)$. As the frequencies tends to the finite value at $h \to h_{sf}$, it follows that $k \sim \sqrt{1-(h/h_{sf})^2}$. At zero field the ratio $\omega_-(0)/\omega_+(0) = k'(0) = k_0'$. The lower frequency equal to $\omega_-(0) \approx 23.8$ GHz (line A in Fig. 4) and weakly depends on temperature [4]. The upper frequency (line C in Fig. 4) strongly depends on the temperature (see Fig. 6 in [5] and an extension of this dependence to $T \to 0$ (line C′ in Fig. 4) gives the value $\omega_+(0) \approx 34$ GHz. (In Fig. 3b the results are given for $T = 4.2$ K with $\omega_+(0) \approx 27.58$ GHz.) From the foregoing formulae, it follows that $k_0' \approx 0.7$ and $k_0 \approx 0.714$. The relation $\omega_-(0) \approx 23.8\ \mathrm{GHz} = \sqrt{2J\beta_1}\,k_0'/k_0 = h_{sf}k_0'/k_0$ leads to the values $h_{sf} \approx 8.67$ kOe and $\beta_1 \approx 0.065$ kOe close to the experimental data from [4]. The resonant frequency in the critical field $h = h_{sf}$ is equal to $\omega_0 \approx 27.6$ GHz.

To obtain the helix period dependence on the external field $L = L(h)$ it is necessary to find the dependence $k = k(h)$. Using obtained from the experiment the approximation $\omega_-(h) \approx \omega_-(0)(1 + 0.16(h/h_{sf})^2)$ for the frequency of the lower branch and the formula (17) it is easy to get the necessary relation

$$k \approx k_0\sqrt{\left(1-(h/h_{sf})^2\right)/\left(1-0.35(h/h_{sf})^2\right)}. \quad (19)$$

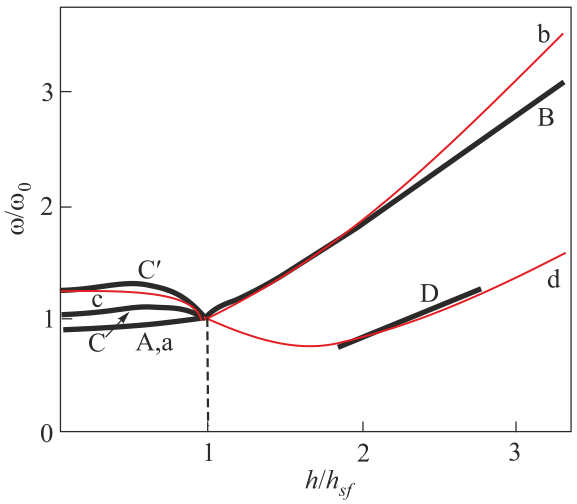

Fig. 4. Theoretical (thin lines b, c, d) and experimental (thick lines) field dependences for the resonance frequencies of helix structure.

Then the theoretical field dependence of the upper branch of AFMR frequency will be (line c in Fig. 4)

$$\omega_+(h) \approx \left(\omega_-(h)/k'\right) =$$

$$= \omega_-(h)\left(1-k_0^2\left(1-\left(h/h_{sf}\right)^2\right)\Big/\left(1-0.35\left(h/h_{sf}\right)^2\right)\right)^{-1/2}. \quad (20)$$

The obtained theoretical results for these AFMR frequency dependences $\omega_+(h)$ and $\omega_-(h)$ are in good agreement with the experimental data (see the lines A, C′ and a, c in Fig. 4). Some discrepancy consists in monotonic decreasing of the frequency with the field in theoretical formula (20). The knowledge of the dependence (19) for $k = k(h)$ gives the final changing of the spiral period:

$$L(h)/L(0) = kK(k)/\left(k_0 K(k_0)\sqrt{1-\left(h/h_{sf}\right)^2}\right) \approx$$

$$\approx 0.75kK(k)/\sqrt{1-\left(h/h_{sf}\right)^2}. \quad (21)$$

It is the function slightly growing with $L(h_{sf})/L(0) \approx 1.045$. In the limit $h \to h_{sf}$ the incommensurate structure transforms into linear helix $\varphi \approx 1.13\, z/\Lambda$ (see the left segment in Fig. 5).

5. Resonant properties of spiral structure in the field $h > h_{sf}$

In fields larger than the field of the spin-flop transition $h > h_{sf}$, the resonance dependences also differ essentially in the case of the collinear phase at high temperatures ($T = 14.6$ K is the line of triangles in Fig. 3b) and at low temperatures ($T = 4.2$ K is the line D in Fig. 3b). Therefore, it is natural to assume that even at $h > h_{sf}$ the system exists in the incommensurate phase. In this case, the Eq. (16) is modernized in this way:

$$2J^2a^2u_{zz} +$$

$$+\left[\left(\omega^2 - \left(h^2 - 2J\beta_1\right)\right) + 2\left(h^2 - 2J\beta_1\right)\mathrm{cn}^2\left(qz,k\right)\right]u = 0, \quad (22)$$

where $\mathrm{cn}(qz,k)$ is the elliptic Jacobi cosine with modulus k and $q = \sqrt{(h/h_{sf})^2 - 1}/\Lambda k$. Periodic solutions of this equation and the corresponding frequencies are

$$u_- = \mathrm{cn}\left(qz,k\right), \quad \omega_- = \omega_0\sqrt{\left(h/h_{sf}\right)^2 - 1}\, k'/k, \quad (23)$$

$$u_+ = \mathrm{sn}\left(qz,k\right), \quad \omega_+ = \omega_0\sqrt{\left(h/h_{sf}\right)^2 - 1}\,/k. \quad (24)$$

To compare these theoretical formulas with experimental data, we, unfortunately, do not have complete information about the low-frequency behavior of the frequency dependences at frequencies lower 20 GHz. In addition, it can be seen from formulas (23), (24) that, in the limit $h \to h_{sf}$ in which $k \to 0$ and $k' \to 1$, the frequencies of the two branches ω_+ and ω_- must coincide. But in the experiment, the lower resonance branch near the point of the spin-flop transition was not observed. Moreover, at $h \approx 2h_{sf}$ (left end of the line D) the peak of absorption disappears in the experiment.

This indicates more complicated behavior of the incommensurate structure in the region near the point of the spin-flop transition. (Note that the term “spin-flop transition” is conditional in the case of an incommensurate structure — the antiferromagnetism vector does not jump abruptly in the corresponding field, but there is a continuous change in the magnetization rotation in the spiral. However, the characteristics of the spiral in this field change significantly.) Nevertheless, we compare the theoretical dependences (23), (24) with the experimental dependences (lines B and D in Figs. 3b and 4).

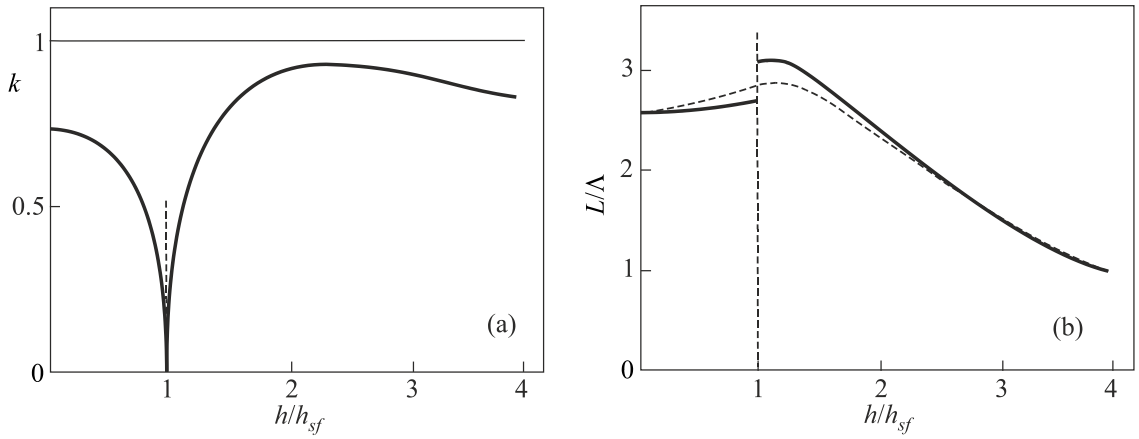

Fig. 5. Field dependences of the modulus of elliptic functions (a) and of the period of the spiral structure (b). The dashed curve in (b) corresponds to a smoothed dependence.

First of all, from (23), (24) it follows the dependence

$$k' = \omega_-(h)/\omega_+(h) \quad (25)$$

for the parameter of the spiral structure on the experimental dependences of the resonant frequencies on the external field. We use the asymptotic behavior of these linear dependences in the fields $h >> h_{sf}$ from [4]: $\omega_+ \approx 24.36(h/h_{sf})$ GHz and $\omega_- \approx (15.52(h/h_{sf}) - 10)$ GHz. From these formulas we obtain the following asymptotic dependences of the modulus of the elliptic function: $k' \approx 0.64 - 0.41(h_{sf}/h)$ and $k' \approx 0.77 - 0.34(h_{sf}/h)$ in large fields $h >> h_{sf}$. In fields larger than the spin-flop field, the expression for the period of an incommensurate structure is modified as follows:

$$L = \Delta 2kK(k)/\sqrt{(h/h_{sf})^2 - 1}. \quad (26)$$

For the indicated relation between the parameter k and the magnetic field, the helix period rapidly decreases ($\sim 1/h$) with the increasing field at large fields (asymptotic behavior in Fig. 5b.

From relations (23), (24) it also follows such a relationship of the resonant frequencies of the two branches of the spectrum

$$\omega_+(h)/\omega_0 = \sqrt{(h/h_{sf})^2 - 1 + \omega_-^2(h)/\omega_0^2}. \quad (27)$$

Taking into account the experimental result for the asymptotic behavior of the ratio $\lim(\omega_+/\omega_-) \approx 1.57$ in large fields and relation (27), we obtain the asymptotic field dependences of the two branches $\omega_+/\omega_0 \approx 1.3h/h_{sf}$ and $\omega_-/\omega_0 \approx 0.83h/h_{sf}$, which are close to the above experimental dependences. Using these asymptotics, the condition $\omega_+(h_{sf})/\omega_0 = \omega_-(h_{sf})/\omega_0 = 1$, the simplest polynomial approximation for the field dependence and the condition for the proximity of theoretical and experimental dependences (using only one fitting parameter), we obtain the following theoretical formulae for the field dependences of two branches of the absorption spectrum:

$$(\omega_-/\omega_0)^2 \approx 0.69(h/h_{sf})^2 - 2.48(h/h_{sf}) + 2.8, \quad (28)$$

$$(\omega_+/\omega_0)^2 \approx 1.69(h/h_{sf})^2 - 2.48(h/h_{sf}) + 1.8. \quad (29)$$

They are shown in Fig. 4 in the form of lines b and d. One can see the good qualitative and quantitative agreement with the corresponding experimental dependences B and D. Note that the theoretical dependence (line b) formally corresponds to zero temperature. At the same time, the experimental curve B was obtained at $T = 4.2$ K. As noted above, with decreasing temperature, the frequencies of the upper branch increase, and with decreasing temperature, agreement with theory should improve. We also note a certain discrepancy between the theoretical and experimental dependences in the used approximation in a narrow region near the spin-flop field. The module of elliptic functions describing the spiral structure is related to the field dependence of the resonance frequencies by the relation

$$k^2 = \left((h/h_{sf})^2 - 1\right)(\omega_0/\omega_+(h))^2$$

and its field dependence, which follows from (28), is approximated by the function

$$k^2 \approx \frac{(h/h_{sf})^2 - 1}{1.69(h/h_{sf})^2 - 2.48(h/h_{sf}) + 1.8}. \quad (30)$$

The full dependence of the modulus of elliptic functions on the amplitude of the field (including the above dependence in the fields $h < h_{sf}$) is shown in Fig. 5a.

The dependence $k = k(h)$ has the root singularities at the spin-flop point, reaches the value $k(0) \approx 0.714$ in zero field, has a maximum with $k = 0.92$ in the field $h/h_{sf} = 2.4$, and decreases in large fields to its asymptotic value $k(h >> h_{sf}) \to 0.77$. A knowledge of the full dependence $k = k(h)$ allows us to use the formula (26) to restore the field dependence of the periods of the spiral structure in the whole interval of the field magnitude. It is shown in Fig. 5b. The discrepancy at the point $h = h_{sf}$ is related to the approximation of the approximating function for fields close to the spin-flop field. This weak discrepancy between the lines b and B is visible in Fig. 4. The dashed curve in Fig. 5b corresponds to a smoothed dependence.

6. Conclusion

The eigenmodes of vibration of spiral structures in magnetic systems, which manifest themselves in their resonance properties, are considered in the work. The external field significantly affects on the structure of such incommensurate systems and their properties. The nature of this influence can be judged by the experimental data obtained by the AFMR method when studying the resonance properties of complex multiferroics. The use of the experimentally obtained field dependences of the resonant frequencies on the magnetic field in combination with a theoretical study of the problem within the framework of a simple model made it possible to obtain information about the changing in the period of the magnetic helicoidal structure with the magnitude of the external field. So far, such dependences have not been obtained using other methods. It is shown that although the classical spin-flop transition in the magnetic field does not occur in the spiral structure, a strong rearrangement of the spiral structure and its properties is observed at a certain critical field associated with the magnetic anisotropy of the crystal. However, some resonant properties of spiral structures observed experimentally, such as the different nature of the absorption for the rf

field with a direct and reverse change in its frequency in the upper branch of the absorption line at $h < h_{sf}$ and the disappearance of absorption on the lower branch near h_{sf} when $h > h_{sf}$, have no theoretical explanation. It is possible that some features of the AFMR for magnetic spirals are associated with the modulation instability of their nonlinear internal modes.

The author is grateful to M.I. Kobets for numerous discussions of the experimental aspect of the problem and for putting in my disposal the AFMR experimental data for $NdFe_3(BO_3)_4$.

This work was supported by the scientific project of the National Academy of Sciences of Ukraine No. 4.17-N and the scientific program 1.4.10.26/F-26-4.

1. Y. Tokura, S. Seki, and N. Nagaosa, *Rep. Prog. Phys.* **77**, 076501 (2014).
2. R. Ramesh and N.A. Spaldin, *Nat. Mater*. **6**, 21 (2007).
3. A.M. Kadomtseva, Yu.F. Popov, S.S. Krotov, G.P. Vorob'ev, E.A. Popova, A.K. Zvezdin, and L.N. Bezmaternykh, *Fiz. Nizk. Tem*p. **31**, 1059 (2005) [*Low Temp. Phys*. **31**, 807 (2005)].
4. M.I. Kobets, K.G. Dergachev, E.N. Khatsko, S.L. Gnatchenko, L.N. Bezmaternykh, and V. L. Temerov, *Physica B* **406**, 3430 (2011).
5. M.I. Kobets, K.G. Dergachev, A.S. Kovalev, S.L. Gnatchenko, and E.N. Khatsko, *Fiz. Nizk. Temp.* **43**, 193 (2014) [*Low Temp. Phys.* **43**, 151 (2014)].
6. M.N. Popova, E.P. Chukalina, T.N. Stanislavchuk, B.Z. Malkin, A.R. Zakirov, E. Antic-Fidancev, E.A. Popova, L.N. Bezmaternykh. and V.L. Temerov, *Phys. Rev. B* **75**, 224435 (2007).
7. M. Janoschek, P. Fischer, J. Schefer, B. Roessli, V. Pomjakushin, M. Meven, V. Petricek, G. Petrakovskii, and L. Bezmaternikh, *Phys. Rev. B* **81**, 094429 (2010).
8. P. Fischer, V. Pomjarushin, D. Sheptyakov, B. Roessli, V. Pomjakushin, M. Meven, V. Petricek, G. Petrakovskii, and L. Bezmaternikh, *J. Phys.: Condens. Matter* **18**, 7975 (2006).
9. S. Hayashida, M. Soda, S. Itoh, T. Yokoo, K. Ohgushi, D. Kawana, and T. Masuda, *Phys. Procedia* **75**, 127 (2015).
10. J.E. Hamann-Borrero, M. Philipp, O. Kataeva, M. v. Zimmermann, J. Geck, R. Klingeler, A. Vasiliev, L. Bezmaternykh, B. Büchner, and C. Hess, *Phys. Rev B* **82**, 094411 (2010).
11. A.M. Kadomtseva, Yu.F. Popov, G.P. Vorobjov, A.P. Pyatakov, S.S. Krotov, K.I. Kamilov, V.Yu. Ivanov, A.A. Mukhin, A.K. Zvezdin, A.M. Kuz'menko, L.N. Bezmaternykh, I.A. Gudim, and V.L. Temerov, *Fiz. Nizk. Temp.* **36**, 640 (2010) [*Low Temp. Phys*. **36**, 511 (2010)].
12. A.K. Zvezdin, G.P. Vorobjov, A.M. Kadomtseva, Yu.F. Popov, A.P. Pyatakov, L.N. Bezmaternykh, A.V. Kuvardin, and E.A. Popova, *Pis'ma Zh. Éksp. Teor. Fiz*. **83**, 600 (2006) [*JETP Lett*. **83**, 509 (2006)].
13. E.S. Borovik, V.V. Eremenko, and A.S. Milner, *Lectures in Magnetism*, M. Fismatlit, Moscow (2005) (in Russian).
14. E.V. Zarochencev and V.A. Popov, *Ukr. Phys. J.* **10**, 369 (1965).
15. D.V. Volkov, A.A. Demidov, and N.P. Kolmakova, *Zh. Éksp. Teor. Fiz*. **131**, 1030 (2007) [*JETP* **104,** 897 (2007)].
16. E.A. Popova, N. Tristan, H. Hess, R. Klingeler, B. Büchner, L. N. Bezmaternykh, V. L. Temerov, and A. N. Vasil'ev, *Zh. Éksp. Teor. Fiz.* **132**, 121 (2007) [*JETP* **105**, 105 (2007)].
17. I.V. Bar'yakhtar and B.A. Ivanov, *Nonlinear Magnetization Waves in Antiferromagnets,* Preprint DonFTI-80-4b, **61** (1980).
18. G.A. Zvyagina, K.R. Zhekov, I.V. Bilych, A.A. Zvyagin, I.A. Gudim, and V.L. Temerov, *Fiz. Nizk. Temp.* **37**, 1269 (2011) [*Low Temp. Phys*. **37**, 1010 (2011)].

Резонансні властивості магнітних гелікоїдальних структур

О.С. Ковальов

Теоретично досліджено залежність від зовнішнього магнітного поля частот внутрішніх мод спіральних структур легкоплощинних антиферомагнетиків зі слабкою внутрішньоплощинною анізотропією в широкому інтервалі полів, що включає поле спін-флоп переходу. Порівняння теоретичних результатів з відомими експериментальними даними по антиферомагнітному резонансу в $NdFe_3(BO_3)_4$ дало можливість встановити залежність кроку спіральної структури від величини зовнішнього магнітного поля.

Ключові слова: антиферомагнетик, антиферомагнітний резонанс, спіраль, моди збуджень..